JPhys Materials

PURPOSE-LED PUBLISHING™

PERSPECTIVE • **OPEN ACCESS**

Viscoelastic ordering in microfluidic devices: current knowledge, open questions and challenges

To cite this article: Francesco Del Giudice and Gaetano D'Avino 2025 *J. Phys. Mater.* **8** 011001

IOP Publishing J. Phys. Mater. 8 (2025) 011001 https://doi.org/10.1088/2515-7639/ad9634

Journal of Physics: Materials

OPEN ACCESS

RECEIVED
14 August 2024

REVISED
24 October 2024

ACCEPTED FOR PUBLICATION
22 November 2024

PUBLISHED
2 December 2024

PERSPECTIVE

Viscoelastic ordering in microfluidic devices: current knowledge, open questions and challenges

Francesco Del Giudice[1,*] **and Gaetano D'Avino**[2]

[1] Complex Fluids Research Group, Department of Chemical Engineering, Swansea University, Fabian Way, SA1 8EN Swansea, United Kingdom

[2] Dipartimento di Ingegneria Chimica, dei Materiali e della Produzione Industriale, Universitá degli Studi di Napoli Federico II, Piazzale Tecchio 80, 80125 Napoli, Italy

[*] Author to whom any correspondence should be addressed.

E-mail: francesco.delgiudice@swansea.ac.uk

Keywords: microfluidics, viscoelastic ordering, microfluidic crystals

Abstract

Objects flowing in microfluidic devices can self-organise in ordered structures thanks to the hydrodynamic interactions mediated by either inertial or viscoelastic forces. Such structures have been found to be crucial to enhancing microfluidic applications such as single encapsulation, co-encapsulation, and material synthesis. However, while inertial ordering has been investigated in more detail, studies on viscoelastic ordering are much more limited. In this perspective, we report the recent advancements in viscoelastic ordering while also discussing the open questions and challenges related to this field. We also include a brief description of both experimental and numerical protocols that can be employed to investigate viscoelastic ordering.

1. Introduction

Ordering in microfluidic devices is the physical phenomenon for which flowing objects, either particles or cells, self-organise in equally-spaced structures during the flow (figure 1). This phenomenon has been observed in either inertia-dominated (figure 1(a)) or viscoelasticity-dominated flows (figure 1(b)) [1]. Microfluidic ordering has only been observed when the number of flowing objects is sufficiently large to enable hydrodynamic interactions to take place. Such interactions are then mediated by the inertial or viscoelastic forces, possibly leading to the formation of equally-spaced structures.

Ordering is generally anticipated by *cross-stream migration* [2–6], i.e. the phenomenon for which flowing objects move transversely to the flow direction in order to occupy specific equilibrium positions. In fact, when entering the microfluidic device, the objects are randomly distributed along the cross-section. Once they reach the equilibrium positions via lateral migration, hydrodynamic interactions begin to take place, thus leading to the ordering phenomenon [1].

As previously mentioned, ordering has been observed when the flow is either inertia- or viscoelasticity-dominated [1]. While inertial ordering has been studied in more detail by both experiments and numerical simulations, viscoelastic ordering remains largely unexplored. There are some advantages of viscoelastic ordering compared to inertial ordering, the most relevant being that viscoelastic ordering promotes the formation of ordered structures arranged on a single line located at the channel centreline (figure 1(b)), where the velocity is maximum, and the shear stress is minimum. To achieve a single-line ordered structure through inertial effects, complex geometries are needed [7, 8], otherwise the ordering occurs on multiple lines [9–11]. In both cases, the objects are ordered next to the wall, where the shear stress is maximum, resulting in possible damage of delicate cells.

The goal of this perspective is multi-fold. First, we want to provide an overview of the current knowledge about viscoelastic ordering based on published works in the past few years. Second, we want to discuss the open questions and the challenges on the ordering phenomenon. Finally, with the aim of promoting further studies on this fascinating subject, we present a summary of both experimental and numerical protocols

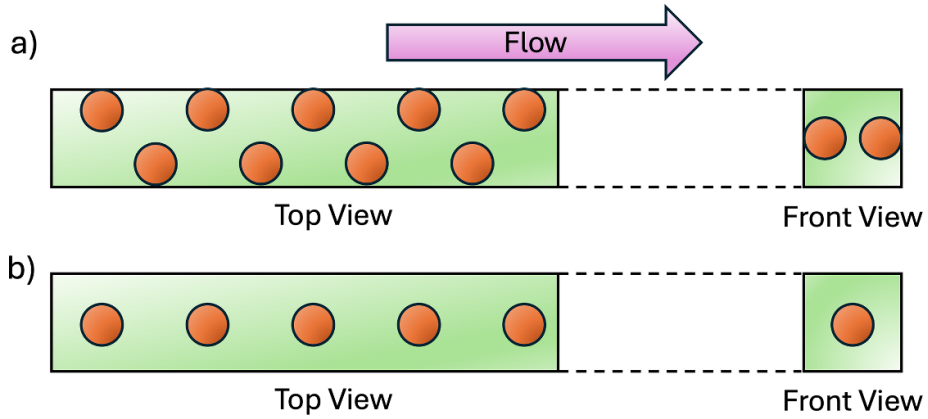

Figure 1. Schematic representation of ordering in microfluidic devices for (a) inertial flow and (b) viscoelastic flow.

required to investigate viscoelastic ordering, providing some guidance to those who are keen to explore this phenomenon.

2. Current knowledge on viscoelastic ordering

We begin by discussing the recent progress in viscoelastic ordering in microfluidic devices. We will first present the impact of fluid rheology and particle/cell concentration on the occurrence of the ordering to then explore the effect of particle and device properties on the observed ordering. We will conclude by summarising how viscoelastic ordering has been used in the context of microfluidic applications.

2.1. Impact of fluid rheology and particle concentration

The first experimental evidence of viscoelastic ordering was reported by Del Giudice *et al* [12]. They employed a solution of hyaluronic acid (HA) polyelectrolyte in phosphate buffer saline (PBS) at 1 wt%. The fluid presented shear-thinning properties and a longest relaxation time estimated to be $\lambda \approx 37$ ms. When the bulk concentration of particles with diameter $d = 20$ μm was $\phi = 0.6$ wt%, the formation of equally-spaced particles in a glass square-shaped capillary with side $H = 100$ μm (i.e. confinement ratio $\beta = d/H = 0.2$) was observed for the flow rate range $10 < Q < 100$ μl min^{-1}, corresponding to a range of Deborah number De$= \lambda Q/H^3$ of $6.2 <$ De < 62 (figure 2(a)). Specifically, particles arranged around the centreline with a characteristic distance $S^* = s/d \approx 3.5$, where s is the distance between consecutive particles. This characteristic distance was independent of the volumetric flow rate and only dependent upon the particle concentration in the channel. Larger values of Q, however, were found to increase the fraction of equally-spaced particles (see the increasing peaks of the distributions in figure 2(a) as De increases). Similar results were also found by Liu *et al* [15], who employed a similar HA solution as suspending liquid for $d = 20$ μm particles flowing in a $H = 100$ μm channel. Their device was different from the one employed by Del Giudice *et al* [12], as it included a series of trapezoidal elements to break up aggregates and a second part to reduce the fluctuation of particle concentration during the experiments. A similar device to break up particle aggregates has also been introduced later [16]. There are a few other experimental works where the ordering phenomenon has been demonstrated using either aqueous solution of xanthan gum (XG) in the concentration range 0.1 wt% to 0.6 wt% [14, 17, 18] and aqueous HA solutions (polymer molecular weight of 1.5–1.8 MDa) in the concentration range 0.1 wt% to 0.5 wt% [15, 19]. Notice that the different rheological behaviour in HA in water and PBS is to be ascribed to the fact that HA is a polyelectrolyte while PBS is a salt that screens the charges on the polymer, thus altering the rheological behaviour of the solution [20, 21].

Viscoelastic ordering was not observed when the suspending liquid presented a near-constant viscosity. In the same work, Del Giudice *et al* [12] reported that using a suspending solution of HA 0.1 wt% (i.e. one order of magnitude smaller in concentration than the solution required for the ordering) in PBS with 25 wt% of glycerol, did not lead to the formation of equally-spaced structures (figure 2(b)). On the contrary, the particles tended to aggregate and form strings of attached particles (see experimental snapshots in figure 2(b)). A similar behaviour was also observed when the suspending liquid was an elastic sodium alginate solution with a near-constant viscosity [22]. From the experimental evidence presented so far, shear-thinning seems to be required to enable viscoelastic ordering. In a series of works, D'Avino *et al* employed numerical simulations to understand the behaviour of interacting particles in viscoelastic liquids (figures 2(c) and (d)) [13, 23, 24]. For the case of two particles suspended in a viscoelastic liquid modelled by

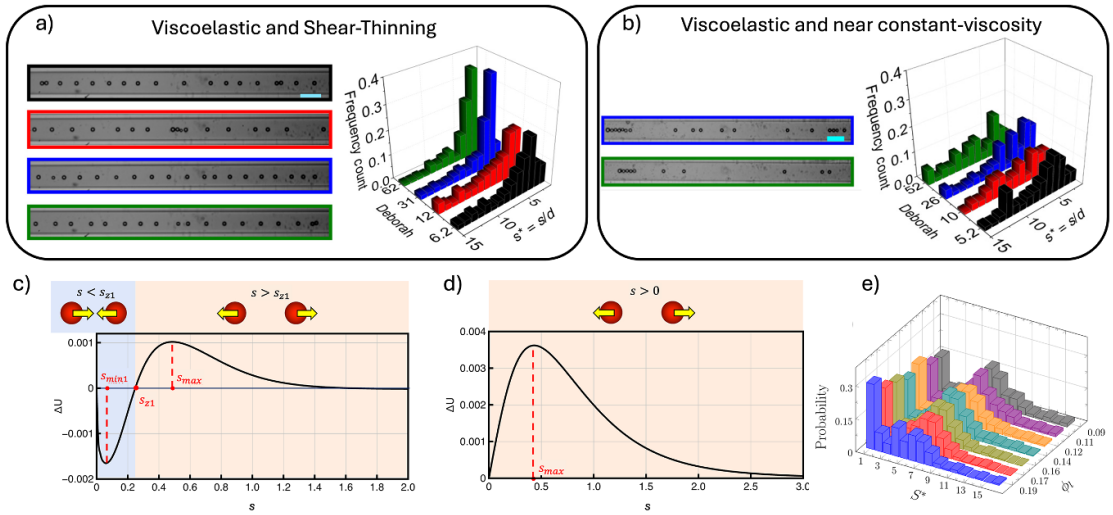

Figure 2. (a)–(b) Experimental snapshots and probability distribution for the distance between consecutive 20 μm particles suspended in a hyaluronic acid solution at 1 wt% in phosphate buffer saline (a) and a hyaluronic acid solution at 0.1 wt% in phosphate buffer saline with the addition of 25 wt% of glycerol (b), flowing in a 100 μm glass capillary. Reprinted with permission from [12], Copyright (2018) by the American Physical Society. (c)–(d) Relative particle velocity as a function of the interparticle distance for a pair of spherical particles aligned along the centerline of a cylindrical channel and suspended in a Giesekus fluid at $\alpha = 0.2$, $\beta = 0.4$ and De$= 0.5$ (c) and De$= 3$ (d). Adapted from [13], with permission from Springer Nature. (e) Probability distribution function for 20 μm particles suspended in a xanthan gum 1 wt% solution in water flowing in a 100 μm glass channel. The concentration $\phi_l = Nd/L$ is the local particle concentration with N the number of particles with diameter d in a channel length L. Reproduced from [14]. CC BY 4.0.

the Giesekus constitutive equation with $\alpha = 0.2$ (i.e. presenting shear-thinning) flowing in a straight circular tube with $\beta = d/D = 0.4$, where D is the tube diameter, different particle dynamics depending on the value of the Deborah number were observed. When De$= 0.5$, i.e. when the fluid explored the near-constant-viscosity region of the flow curve, particles could either attract or repel depending upon their initial distance (figure 2(c)). When the Deborah number was increased above De$= 1$ to De$= 3$ (figure 2(d)), i.e. when the fluid explored the shear-thinning region of the flow curve, only repulsion was observed. The authors also performed numerical simulations for different values of the constitutive parameter α modulating the onset of the shear-thinning behaviour and observed that the smaller the amount of shear-thinning, the larger the possibility of observing particle-particle attraction. These results are in agreement with the simulations by Hu *et al* [25], who found that monodisperse particles suspended in an Oldroyd-B liquid (i.e. a Giesekus model with $\alpha = 0$) enhanced particle-particle attraction.

Particle concentration has an important impact on viscoelastic ordering. Del Giudice *et al* [12] observed that when the solid concentration was too low, then particles did not tend to form equally-spaced structures. This is expected as the entire viscoelastic ordering phenomenon is driven by particle-particle hydrodynamic interactions that cannot take place if the particles are too far apart. When increasing the concentration up to 1 wt%, the formation of doublets disrupting the continuity of the particle train was observed. This is justified by the fact that an increase in particle concentration resulted in particles being closer to each other when entering the channel, and numerical simulations showed that even in shear-thinning liquids, there is the possibility of observing attraction when the particles are close to each other [13, 23, 24]. Particle aggregation was studied in detail by Jeyasountharan *et al* [14] using XG as suspending liquid (figure 2(e)). They observed a significant number of particle doublets, especially when increasing the bulk particle concentration. Additionally, they also observed that by simplifying the connections between the reservoir and the channel, it was possible to significantly reduce the number of aggregates. Another strategy to reduce doublets formation is to break down such aggregates as soon as they form, with the highest probability of this happening being when the particles enter the microfluidic device. To do that, some trapezoidal structures can be introduced to break down aggregates based on the principle of acceleration and deceleration of the fluid with the suspended particles [15, 16, 26]. Particle doublets in XG solutions have also been experimentally observed by Hu *et al* [27].

Taken together, experimental and numerical results presented so far highlighted the need for shear-thinning liquids to observe particle ordering. Also, the particle concentration and the experimental conditions need to be tuned appropriately to i) reduce the occurrence of particle doublets (avoiding high particle concentrations), and ii) have appreciable interparticle hydrodynamics interactions to promote a re-arrangement of the microstructure (avoiding low particle concentrations).

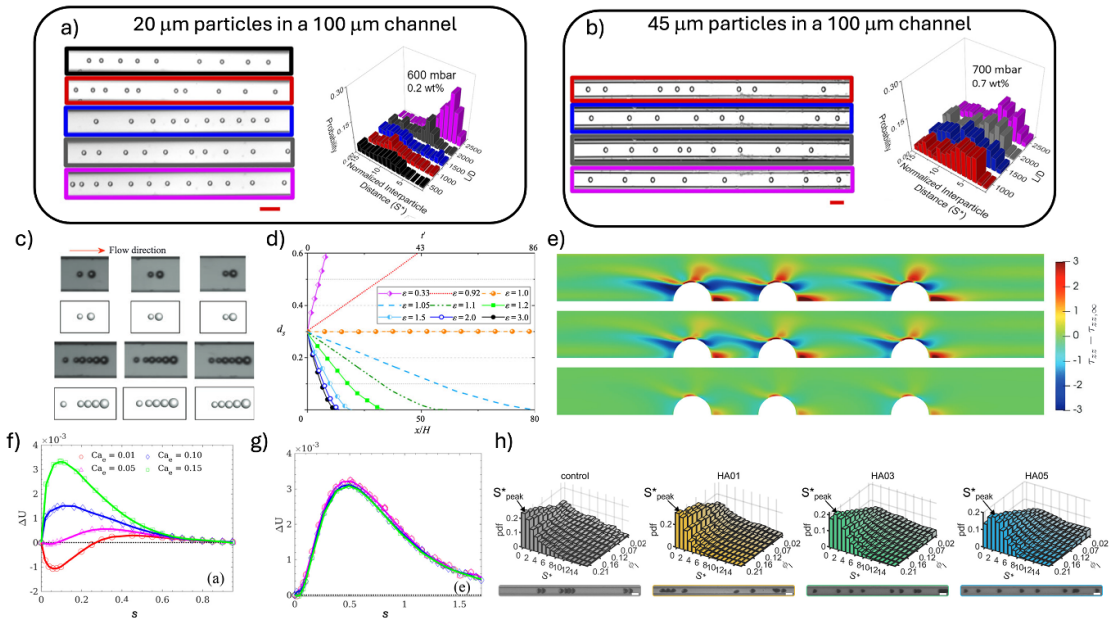

Figure 3. (a)–(b) Experimental snapshots and probability distribution for the distance between consecutive particles suspended in an aqueous xanthan gum 0.1 wt% solution for 20 μm (a) and 45 μm (b). Reproduced from [16]. CC BY 4.0. (c) Experimental (top) and numerical (bottom) results for polydisperse particle systems of 2 and 5 particles. (d) Evolution of spacing of two particles with different diameter ratios. Reproduced with permission from [27]. 2022 © Cambridge University Press, reproduced with permission. (e) Color maps of the difference between the zz-component of the (dimensionless) viscoelastic stress tensor and the same component of the unperturbed fluid for an increasing wall slip from top (corresponding to the no-slip case) to bottom. Reproduced from [28]. CC BY 4.0. (f)–(g) Master curves of the terminal relative velocity between two elastic particles in a viscoelastic medium as a function of the interparticle distance and of the elastic capillary number at $\beta = 0.4$ for De$= 0.125$ (f) and De$= 2$ (g). Adapted from [29], with the permission of AIP Publishing. (h) Experimental snapshots and probability distribution function for the distance between consecutive red blood cells suspended in different viscoelastic liquids. Reproduced from [18]. CC BY 3.0.

2.2. Effect of particles and channel properties

In this section, we focus on the impact of particle and channel properties on the ordering phenomenon. This includes understanding the effect of particle size, shape, polydispersity, wall slip in microchannels and particle/cell deformability.

Particle size and shape

The impact of particle size on the viscoelastic ordering has been studied using both experiments and numerical simulations (figures 3(a) and (b)) by Jeasountharan *et al* [16]. The authors employed XG 0.1 wt% in water as suspending liquid and a glass microchannel having a diameter $D = 100$ μm. When $\beta = 0.2$ (i.e. particles with diameter $d = 20$ μm), ordering was experimentally observed for normalised channel lengths $L/D \geqslant 2000$ (figure 3(a)). When the confinement ratio was increased to $\beta = 0.45$ (i.e. particles with diameter $d = 45$ μm), ordering was observed for $L/D \geqslant 1000$, meaning that an increase of the confinement ratio resulted in a larger number of ordered particles at shorter distances from the channel inlet. The experiments were also supported by numerical simulations that showed a dependence of the relative velocity between a leading and a trailing particle $\Delta U \propto \beta^4$, meaning that the confinement ratio has a very strong impact on the particle ordering. Numerical simulations also confirmed that larger particle concentrations suppressed the ordering even at large values of β, thus reiterating the importance of choosing the particle concentration appropriately. The effect of particle shape remains only studied by numerical simulations for a two particle system [13], with the main result being that two spheroidal particles aligned with major axis along the channel centerline did not experience attraction, no matter the rheology of the fluid. Particle shape is poorly studied even in the context of simple particle migration with only a few works presented on the subject [30–33].

Polydispersity

The impact of polydispersity on particle ordering is very important to understand because of the repercussions on the potential applicability of viscoelastic ordering in biomedical applications, being cells generally heterogeneous. Polydispersity in the context of particle ordering has been studied in detail by Hu *et al* [25, 27]. In their works, the authors observed that if a large particle leads a small one, the two particles tend to attract (figure 3(c)). This is because the small particles flow faster than the larger ones due to

the less effective slowing down effect of the confinement. The same was observed if a large particle leads a series of small particles (figure 3(c)). When the leading particle was smaller than the trailing one, no strings were observed. Additionally, the strings were formed regardless of the suspending liquid rheology, with strong shear-thinning properties accelerating the formation of aggregates. The formation of string was more marked when the Deborah number (defined as $\mathrm{De}= 4\lambda Q/D^3$) was $\mathrm{De}\geqslant 1$. Strings were only observed when the ratio of the diameters of the larger and smaller particles was equal or larger than one (figure 3(d)). The larger the value of this ratio, the quicker particles formed strings. According to the existing evidence, polydispersity seems to have a negative impact on the ordering mechanism, especially considering that shear-thinning, desired for viscoelastic ordering, accelerates string formation.

Wall slip

The effect of wall slip on particle ordering has been recently studied by numerical simulations [28]. Understanding the impact of wall slip on particle ordering is important in the context of single-cell encapsulation [10, 17, 19]. Since biological systems require an aqueous matrix, the droplet should be made out of an aqueous solution. However, to achieve that, a channel with a hydrophobic surface is required, otherwise the droplet cannot form [34]. Aqueous solutions flowing in a hydrophobic channel are subjected to the slip condition, meaning that the fluid does not adhere to the channel wall, thus causing the fluid to 'slip' [28]. D'Avino and Maffettone [28] observed that the ordering efficiency reduced with increasing of wall slip conditions, and longer channels were required to achieve the same level of ordering of the no-slip case. The reduced efficiency of ordering was due to the different profile of the viscoelastic stresses in the fluid between consecutive particles (figure 3(e)). In the no-slip case, there was a maximum of viscoelastic stresses on the right-hand side of the particles (figure 3(e), top). The magnitude of such maximum decreased with increasing the amount of slip (figure 3(e), middle and bottom), meaning that the repulsion dynamics slowed down significantly, thus delaying the viscoelastic ordering phenomenon. The numerical simulations echoed previous experimental results [17], where a reduced ordering efficiency in a hydrophobic glass channel when compared to the hydrophilic version of the same channel was observed.

Deformability

The impact of deformability of the flowing objects has been investigated both via numerical simulations [29] and experiments [18]. Deformability is an important parameter to understand in the context of viscoelastic ordering, as biological systems such as cells are deformable. Numerical simulations studied the impact of particle deformation on the dynamics of pairs of particles suspended in viscoelastic liquids (figures 3(f)–(g)). For $\beta = 0.4$ and $\mathrm{De}= 0.125$, an increase in the particle deformability, quantified by an increase of the elastic capillary number $\mathrm{Ca_e}$, resulted in particles mainly experiencing repulsion (figure 3(f)). For the same conditions, but for low values of $\mathrm{Ca_e}$, particles could also attract, as also observed for rigid particles in viscoelastic liquids [13]. An increase of the Deborah number to $\mathrm{De}= 2$ resulted in particles experiencing repulsion, no matter the deformability of the object (figure 3(g)). In other words, particle deformability has a positive impact on particle repulsion, which is beneficial for viscoelastic ordering. The only experimental evidence of cell ordering has been reported very recently [18]. In their work, the authors observed that fluid presenting shear-thinning properties favoured the formation of equally-spaced red blood cells (RBC, figure 3(h). It is important to notice that, in the case of RBC, the cells occupied almost the entire channel, with a confinement ratio $\beta \approx 0.94$. According to the numerical simulations introduced earlier [16], the ordering phenomenon scaled with β^4; in fact, Rectenwald *et al* [18] observed RBC ordering at $L/D_\mathrm{h} = 125$ (with L and D_h the length and the hydraulic diameter of the channel), in excellent agreement with the scaling predictions. Practically, being the channel hydraulic diameter equal to ≈ 10 μm, the channel length at which the ordering was observed was $L \approx 1.25$ mm, which is a very short channel, ideal for downstream microfluidic applications. The authors also performed numerical simulations that echoed previous results.

In summary, these results showed that increasing the confinement ratio β by either increasing the particle diameter or by reducing the channel size is beneficial for particle ordering. The polydispersity was proven to be detrimental to particle ordering, especially when a larger particle was leading a smaller one. The wall slip on the channel wall delayed the formation of ordered structures. Finally, the deformability of particles and cells was beneficial for particle ordering as it promoted repulsive forces over attractive ones.

2.3. Applications of viscoelastic ordering

In this section, we briefly discuss the applications employing viscoelastic particle ordering. Maisto *et al* [22] coupled the well-established ex-situ ionic gelation process [35, 36] to the viscoelastic ordering phenomenon to generate a new class of materials featuring fibres with equally-spaced particles (figure 4(a)). An aqueous solution of sodium alginate (required to generate the fibres) and HA to enable viscoelastic ordering and to then activate the chemical cross-linking reaction when the liquid became in contact with the calcium

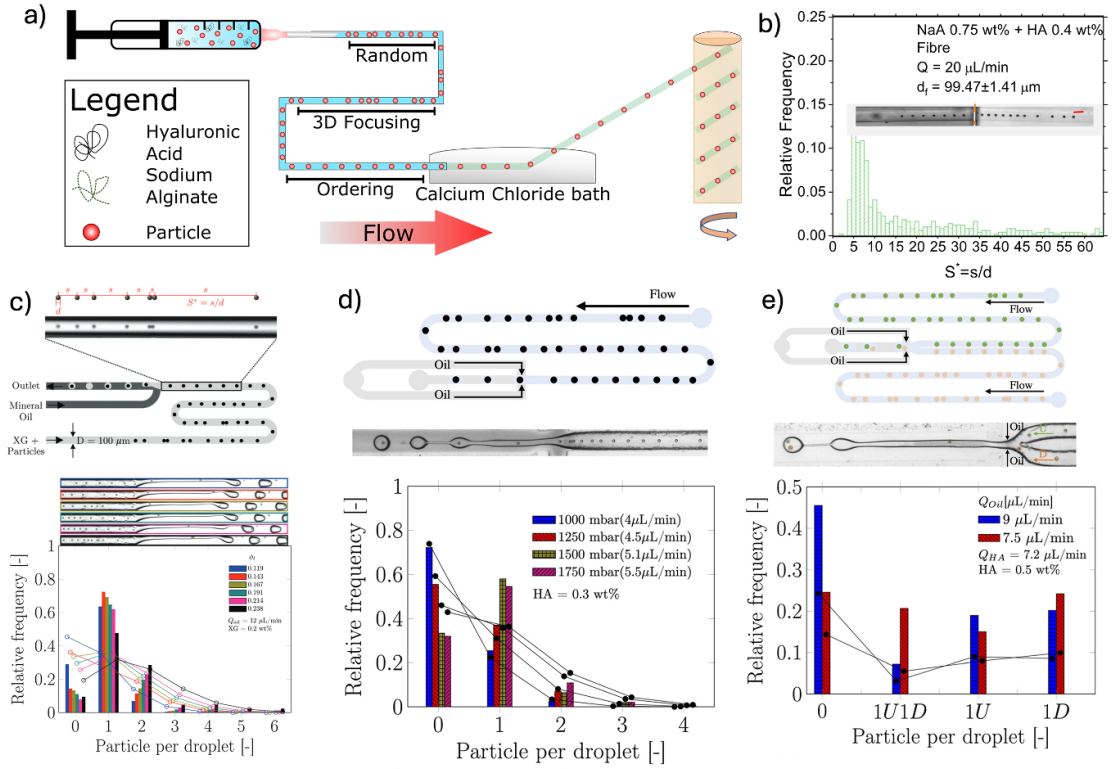

Figure 4. (a) Schematics of the viscoelastic ordering working principle. Particles suspended in an aqueous sodium alginate (NaA) and hyaluronic acid (HA) solution flow into the microfluidic tube. Particles first align on the tube centerline because of the viscoelastic forces acting on them and then self-order thanks to the viscoelasticity-mediated hydrodynamic interactions. (b) Distribution of distances between consecutive particles in a fibre. The experimental snapshot displays the interface between the tube and the calcium chloride bath where the fibre is formed. Reproduced from [22]. CC BY 4.0. (c) Controlled viscoelastic encapsulation in a T-junction device using XG as suspending liquid. Relative frequency of encapsulation, with the observed single particle encapsulation efficiency well above the stochastic value indicated by the connected dots. Reproduced from [17]. CC BY 3.0. (d) Controlled single encapsulation in a flow-focusing device using HA as a suspending liquid. (e) Controlled co-encapsulation in a flow-focusing device demonstrating an efficiency of co-encapsulation of one particle from the upper stream and one from the downstream higher than the stochastic limit indicated by the connected dots. Reproduced from [19]. CC BY 3.0.

chloride bath was employed. The distribution of particles in the tube could either be preserved or not depending on the experimental conditions (figure 4(b)). For instance, increasing the rotational speed of the motor required to spin the fibre resulted in an acceleration of the particles in the fibres due to an overall reduction of the fibre diameter, thus slightly affecting the interparticle distance. Nevertheless, fibres containing equally-spaced particles were successfully manufactured.

The remaining applications are in the field of encapsulation, essential in the context of single-cell analysis. Generally, the encapsulation process is stochastic in nature because the particles can approach the encapsulation area at any time, while the droplets are formed at a constant frequency [9, 10]. The outcome is an encapsulation efficiency of around 30%, which is generally referred to as the 'Poisson limit'. To encapsulate above this limit, Edd *et al* [10] demonstrated the possibility of using inertial ordering to achieve a constant frequency, and then synchronising that frequency to the frequency of droplet generation. The same principle has been used to demonstrate the viscoelasticity-enhanced controlled encapsulation in both T-junction [17, 26] and flow-focusing [19]. In both cases, a hydrophobic channel was required to generate the aqueous droplets [34]. In the T-junction, a long glass channel with hydrophobic coating and with $L/D \geqslant 3500$ was successfully used to order the particle before using mineral oil with Span 80 surfactant to cut the droplets: an encapsulation efficiency up to two folds larger than the Poisson limit was reported (figure 4(c)). To counteract the negative impact of wall-slip on ordering observed in hydrophobic channels [28], the authors increased the concentration of XG compared to the hydrophilic glass channel [14], thus achieving good viscoelastic ordering. Similar performances were achieved by employing a flow-focusing configuration using HA as suspending liquid (figure 4(d)). In the context of Drop-seq [37], a cell must meet a functionalised bead in the same droplet in order to extract the cell mRNA. However, the probability of encapsulating a bead and a cell in the same droplet is limited by the product of two Poisson distributions at around 5% [37]. In this regard, Shahrivar and Del Giudice [19] demonstrated that viscoelastic ordering could be used to improve the encapsulation efficiency up to 25% (figure 4(e)).

In general, the applications related to viscoelastic ordering all remain at a proof-of-concept stage, with future work required to demonstrate their wide applicability to different fields.

3. Open questions and challenges

The train dynamics is governed by the complex hydrodynamic interactions of a multiparticle system. Although the interactions decay at some distance from the particle center, a perturbation of the motion of one particle affects the dynamics of the neighbouring particles so that the disturbance is progressively transmitted along the train. In this complex picture, the pairwise hydrodynamic interactions play a crucial role. As discussed in the previous section, numerical studies [13, 23] have shown two possible scenarios depicted in figures 2(c) and (d). In the former case, an attractive region is found at small distances, followed by a repulsive zone as the distance increases. In the second case, the two particles repel at any distance. The existence of an attractive dynamics is clearly detrimental for ordering as the formation of strings of particles in contact is promoted. Hence, the conditions leading to the second scenario should be preferred. It has to be pointed out, however, that a fully repulsive dynamics does not exclude the formation of particle strings. Indeed, as follows from a qualitative argument on the train stability [12], a particle displaced from its equilibrium position of an ordered structure restores the original position only if the train spacing is higher than the critical distance corresponding to the maximum in figure 2(d), i.e. along the branch of the curve such that the force decreases as the distance increases. In case the train spacing is lower than the critical distance, a perturbation of the particle position from the equilibrium one amplifies and the particle gradually approaches the closest adjacent particle forming a pair. This sets an upper limit for the particle concentration to have an efficient ordering (large concentration values correspond to small equilibrium train spacing).

Hence, understanding the conditions that determine the shape of the relative velocity is crucial to properly design microfluidic devices for particle ordering. Pair particle simulations [13] demonstrated that fluid rheology strongly alters the hydrodynamic interactions. In general, higher elasticity and shear-thinning reduce the attractive region up to disappear. The reason behind this evidence is unclear. The presence of an attractive force at small distances has been attributed to the low axial viscoelastic stresses in the space between the two particles due to the small velocity gradient as the fluid in the gap travels at approximately the same particle velocities [13]. The forces that should separate the particles are then unable to counteract those that tend to approach them acting from the external particle sides, resulting in an attractive dynamics. A similar analysis by varying the fluid rheological properties is missing.

In this regards, it has to be pointed out that the most of the available numerical works have been carried out with the same constitutive equation, i.e. the single-mode Giesekus model. This model predicts the typical rheological features of non-Newtonian fluids such as shear-thinning, first and second normal stresses in shear flow, strain hardening in extensional flow. Along with the relaxation time and the polymer viscosity, this model contains one more parameter (the so-called 'mobility'). By increasing this constitutive parameter, the attraction region in figure 2(c) reduces up to disappear [13]. In shear flow, a larger value of the mobility parameter lowers the shear rate value for the onset of the shear-thinning. On that basis, it has been concluded that fluid shear-thinning helps in preventing pair formation [13, 23]. Whereas this might be true, it has to be remarked that the mobility parameter affects other rheological properties as well. For instance, the entity of strain hardening in elongational flow reduces as the mobility increases, and the flow field around the particles is such that extensional flow might be relevant. The central role of the fluid rheological properties has been recently demonstrated by numerically studying the train dynamics with a different constitutive equation (the Phan-Thien Tanner model) [38]. The main difference with the Giesekus model predictions is the absence of the second normal stress difference. Furthermore, the value of the constitutive parameter adopted in the simulations is such that the shear-thinning behaviour starts at lower values of the shear rate and the strain hardening is much more limited as compared to the Giesekus constitutive equation. The results in terms of ordering are, however, drastically different as the pairing phenomenon is absent and the distributions of the interparticle distances show only one peak that increases as the train travels through the channel, i.e. the particles are gradually self-organizing in an equally-spaced microstructure. A comprehensive study focused on the effect of the fluid rheology from the pair to the train dynamics is then needed to properly select the suspending medium and enhance the ordering efficiency.

Still concerning the fluid rheology, shear-thinning seems to be a necessary condition for particle ordering [12]. As previously mentioned, the attraction region in the pair particle dynamics reduces as the shear-thinning increases. This effect is, however, quantitatively small. Furthermore, the critical distance corresponding to the maximum of figure 2(d) remains substantially unchanged by varying the shear-thinning. Hence, the drastic different behaviour experimentally observed for a constant-viscosity (no ordering) and a shear-thinning (ordering) elastic fluid cannot be completely justified based on the available results.

All the experimental and numerical works have considered viscoelastic liquids as suspending medium. A variety of other complex liquids might be employed as worm-like micellar solutions or elastoviscoplastic materials. In the latter case, in a pressure-driven cylindrical channel, the existence of a yield-stress (i.e. a threshold for the level of applied stress below or above which the material behaves like a solid or a liquid [39, 40]) is responsible for a central solid-like region (unyielded region) travelling as a plug surrounded by a liquid annulus (yielded region). Such a plug region strongly alters the dynamics of particles as recently reported by numerical simulations [41]. Specifically, a neutrally buoyant rigid spherical particle initially embedded in the core region translates at the same velocity of the plug without migrating and rotating. In contrast, particles released in the fluid region migrate within this region towards an equilibrium position between the centreline and the closest wall. Such an equilibrium position shifts towards the wall as the yield-stress increases since the solid-like region expands. Interestingly, when both elasticity and plasticity are relevant, the particle can enter the plug region and move towards the centerline. Once aligned, it is likely that the particles interact hydrodynamically differently from the viscoelastic case, as reported for two bubbles sedimenting in an elastoviscoplastic liquid [42] and two rigid particles in a sheared yield-stress material [43]. A relevant parameter is the width of the unyielded region. For a sufficiently large yield-stress, the plug region can fully embed the particles and any relative motion is suppressed (or extremely slowed down). In this case, the microstructure is 'frozen' and no ordering is expected. If the particles are only partially included in the unyielded region, a relative motion of the particles might be possible and further investigation is needed to derive diagrams like those in figures 2(c) and (d).

The experimental conditions adopted to investigate viscoelastic ordering are such that the Reynolds number (defined as $\mathrm{Re}=\rho UH/\eta$, with ρ and η the fluid density and viscosity, U the average fluid velocity and H the channel size) is much lower than unity so inertia is negligible and the train dynamics is governed by purely elastic effects. The available numerical studies follow this assumption by setting $\mathrm{Re}=0$. However, the formation of an ordered microstructure is also observed for a Newtonian suspension flowing in a microchannel at finite Reynolds number [8, 10, 44–46]. In this case, a stable configuration of the train is the 'staggered' structure, i.e. the particles are located between the channel centerplane and the two lateral walls arranged in a zig-zag pattern [8, 45, 46]. Linear trains have been also experimentally observed along a streamline between the channel center and the wall, although it is unclear whether this configuration is stable [46–48]. Since viscoelasticity promotes centerline alignment and inertia allows an efficient spacing, it would be interesting to investigate the ordering mechanism in an inertio-elastic regime, i.e. under conditions such that both elasticity and inertia are relevant. This is already exploited in particle migration where an efficient 3D focusing [49, 50] and separation [51, 52] can be achieved by using viscoelastic fluids at finite Reynolds numbers.

As discussed in the previous section, particle shape has a relevant effect on the ordering dynamics. With the exception of a couple of recent works dealing with deformable particles, the available studies have been focused on rigid spherical inclusions. However, the shape of the suspended particles can differ from the sphere especially in biological applications. Fluid viscoelasticity has been proven to focus at the channel centerline spheroidal (and in general axisymmetric) particles as well [30, 32, 33, 52–55]. Indeed, by properly setting the Deborah number, a single line of particles oriented with major axis along the flow direction can be obtained [33, 53]. How the train of anisotropic particles evolves and how the dynamics differs from spheres is unknown. Results of pairwise interactions show that the tip of the particles increases the viscoelastic stresses in the space between the two particles, generating a repulsive force that prevents attraction under the same conditions when two spheres attract each other [13]. In addition, the critical distance corresponding to the maximum relative velocity in figure 2(d) moves at lower values as the aspect ratio of the particles increase [13]. Both evidences promote the formation of ordered structures with a reduced formation of strings of particles in contact, thus making this analysis worth of investigation.

An unsolved issue is the formation of particle strings. This problem has been alleviated by using a series of trapezoidal elements between the focusing and the ordering channel sections [16], reducing particle aggregates down to 5% of the overall particle number. Although the aggregate break-up is beneficial for ordering, the addition of trapezoidal elements make the design of the device more complex and much longer (in Jeyasountharan *et al* [16] the length of the trapezoidal element section was about 20 cm followed by a 30 cm channel for ordering). The analysis of the flow field, assuming a Newtonian fluid without particles, shows that the velocity profile first decreases when the fluid enters each element and subsequently increases, leading to the breakage of particle aggregates [15]. However, the effect of the shape of the elements has not been investigated. A systematic fluid dynamics study, taking into account the elasticity of the fluid and the presence of particles (which significantly alter the flow field), is needed to optimize the element shape and analyse different geometries. Notice that, despite the aggregate breakage is beneficial for ordering, the pairing phenomenon can still take place if two particles are close enough when entering the ordering channel section. Indeed, the train microstructure in inlet has been proven to have a crucial effect on ordering.

Specifically, if the minimum distance between the particles is above a threshold, all the particles self-assembly towards an equally-spaced structure without string formation [24]. This result suggests that, along with aggregate breakage, the channel should be designed to increase the distance of the particles as well. As previously mentioned, apart from structural modifications of the device, string formation might be reduced by properly selecting the suspending liquid or by combining inertial and elastic effects.

4. Experimental and numerical approach

In this section, we describe both experimental and numerical protocols previously employed to perform viscoelastic ordering studies. The scope is to provide some easy guidelines with a methodology based on our previous experience.

4.1. Experimental protocol

Suspending fluids

To promote viscoelastic ordering, a shear-thinning fluid seems to be required. The most suitable fluid for viscoelastic ordering studies has been HA in aqueous solutions at mass concentrations larger than 0.1 wt%. HA has been tested in several microfluidic devices made of polydimethylsiloxane (PDMS) [15, 26, 27], polymethylmethacrylate (PMMA) [19] and glass [12]. Xanthan gum (XG) has also been previously used at concentrations above 0.1 wt%, however, its shelf-life is short, and the sample needs to be prepared fresh immediately after 24/48 h. Moreover, XG has been successfully used in glass only [14, 16, 17], while particles tended to migrate towards the wall when using PDMS [27]. We also observed a similar trend with XG in PDMS and PMMA devices (data not published), thus suggesting that XG tends to work only in glass devices for reasons that are not yet clear. Very recently, polyethylene oxide with a molecular weight of 4 MDa has also been successfully used in PDMS devices at the concentration of 1 wt% for RBC at confinement ratio $\beta \approx 0.94\%$ [18]. It is important to point out that, when using a PDMS device, some care must be taken in observing whether the large volumetric flow rate and wall shear stress cause swelling of the channel wall [56], resulting in a 'larger' channel width with consequently a smaller β and a negative impact on ordering. For this reason, channels made of a rigid material, such as glass and PMMA, are to be preferred.

Microfluidic device and particles sizes

The viscoelastic ordering in simple straight channels requires relatively long distances to develop depending on the confinement ratio β. So far, ordering has only been observed when $\beta \geqslant 0.2$ because, otherwise, particles would tend to migrate towards the wall in a shear-thinning liquid [57]. For $\beta = 0.2$, a normalised channel length $L/D \geqslant 3000$ is required when operating with volumetric flow rate values between 1 μl min^{-1} and 20 μl min^{-1}. If, instead, the flow rate can be increased to 50 μl min^{-1}, even a value of $L/D \approx 800$ has been found to be suitable [12]. When increasing the confinement ratio to $\beta = 0.45$, the required normalised length dropped to $L/D \geqslant 1000$ when operating with volumetric flow rate values between 1 μl min^{-1} and 5 μ min^{-1}.

In terms of channel design, it is suggested to add an initial inlet area such as the one we introduced earlier [12] because it seems to reduce the fluctuation of flowing particles. The addition of trapezoidal elements after this initial area has been shown to drastically reduce the number of aggregates [15, 16]. An additional structure to facilitate particle redistribution has also been found to improve the ordering [15]. These additional sections need to be implemented before the long channel where the particle ordering takes place.

Particle concentration

Particle concentration needs to be sufficiently large to enable hydrodynamic interactions. So far, particle concentrations employed have been generally above 0.2 wt% for 20 μm particles and 0.7 wt% for 45 μm particles. Of course, these concentration values are a first attempt, and from experimental observation it should be possible to appreciate whereas there are too many or not enough particles flowing on the channel centreline.

4.2. Numerical methods and strategies

The simulation of the train dynamics involves the motion of a very large number of particles. As an example, for a confinement ratio of $\beta = 0.4$ and a linear concentration $\phi_l = Nd/L = 0.1$ with N the number of particles with diameter d in a channel length L (corresponding to a center-to-center distance of 10 particle diameters), an average of 250 particles travels in a channel with $L/D = 1000$. A direct numerical simulation (DNS) approach, i.e. the solution of the fluid dynamics governing equations (mass and momentum balance equations together a constitutive equation for the liquid) is unfeasible even in an axisymmetric domain due

to huge computational resources required. Furthermore, the relative velocity between two consecutive particles, which must be accurately computed as it governs the train dynamics, turns out to be very small (two or three order of magnitudes lower than the fluid average velocity). Hence, an extremely refined mesh surrounding the particles is needed, further increasing the computational cost.

To overcome these issues, a two-step approach has been proposed based on the assumption that each particle of the train hydrodynamically interacts only with the leading and trailing ones [12, 24]. This assumption has been proven to be an acceptable approximation as, due to the single-line arrangement, the leading and trailing particles 'shield' the hydrodynamic interactions with the other particles of the train. As consequence of this assumption, the train can be decomposed in a set of several three-particle systems. Hence, the first step of the simulation approach is to investigate a system made of three particles already aligned at the channel centerline through DNS. In particular, by varying the interparticle distances, the three particle velocities are computed and stored in a look-up table. Notice that the velocities are stored after the initial viscoelastic stress build-up. The second simulation step consists in solving a kinematic equation $\mathrm{d}z_i/\mathrm{d}t = V_i$ for each particle with z_i and V_i its axial position and axial translational velocity. The latter quantity only depends on the distance between the ith particle and the trailing and leading ones, and is computed by interpolating the data of the look-up table. In this way, the largest computational cost is in generating the look-up table, whereas the train dynamics involving thousands of particles is computed very fast.

Regarding the DNS step, as previously remarked, an accurate solution of the velocity and stress fields around the particles is needed to properly evaluate the particle relative velocities. A boundary-fitted mesh together with the arbitrary Lagrangian Eulerian formulation [58] has been proven to be a good choice [12, 24]. Methods employing a structured grid like the immersed boundary lattice Boltzmann method with an adaptive mesh refinement [59, 60] can be other options. Finally, to overcome the numerical difficulties related to the viscoelastic constitutive equations, it is recommended to employ stabilization techniques like the Streamline-Upwind Petrov-Galerkin formulation [61] and the log-representation for the conformation tensor [62, 63], especially at high values of the Deborah number.

5. Conclusions and outlook

We summarised the current understanding of viscoelastic ordering while discussing the outstanding issues. Experiments and numerical investigations have both been carried out with the aim of understanding the dynamics of the ordering. Experimentally, the existing works have demonstrated the occurrence of particle ordering when the suspending liquid is shear-thinning while also investigating the impact of the confinement ratio, fluid properties and polydispersity. More work has instead been carried out with numerical simulations, where it was found that the repulsive forces between consecutive flowing objects required to achieve ordering were facilitated by large Deborah numbers and strongly shear-thinning liquids. Deformability seemed to aid particle ordering because it promoted repulsive forces, and experimental evidence of cell ordering has also been presented. Regarding microfluidic device design, some care must be taken, with the introduction of adjusted inlets and other structures to reduce particle aggregates and the fluctuation of incoming particles, which is essential to facilitate the ordering.

Several questions are still open. First of all, why shear-thinning is essential for ordering is unexplained. More in general, the effect of other rheological features (e.g. viscoplasticity, extensional properties) might be important and has not been explored yet. In this direction, numerical simulations could be helpful due to the flexibility to choose constitutive equations with different rheological properties. Similarly, most of the viscoelastic solutions employed so far are polyelectrolyte (e.g. Xanthan Gum and HA). The viscoelastic properties of those systems strongly depend upon ionic strength and pH, which can be tuned by changing the type and concentration of dissolved salts [20]. We are not aware of a study elucidating the impact of such parameters on the ordering, aside from the expected ones relating the ordering efficiency to the shear-thinning properties of the solutions. This is especially important in single-cell encapsulation where cell media (containing salt) is essential for the cells to survive. Particle shape is limited to spheres. The analysis of pairwise interactions shows that spheroids are less prone to form strings as compared to spheres, thus promoting the ordering mechanism, which obvious interest in biological applications. A critical issue is, indeed, the pairing phenomenon, i.e. the formation of structures made of particles in contact. A remedy has been proposed by using an array of elements with variable cross-section upstream the channel where ordering takes place aimed at breaking-up possible aggregates. The number and the shape of elements might be not optimal and a comprehensive fluid dynamics study is needed. Furthermore, the absence of aggregates does not prevent the pairing phenomenon unless the particles are sufficiently separated. This motivates further investigation on this topic, for instance by considering the effect of inertia along with elasticity that might also be beneficial in speeding-up the ordering dynamics.

In terms of applications, the works available so far are limited to material synthesis, controlled encapsulation and co-encapsulation, with both strategies at the proof-of-concept stage. More recently, the ordering phenomenon has been exploited to estimate the fluid relaxation time through machine learning techniques, although the study is limited to *in silico*-generated datasets [64]. Furthermore, the good performances obtained in terms of classification and regression are related to a specific constitutive equation used to generate the dataset. A more comprehensive and general study would be to include the effect of the constitutive parameters and of the rheological constitutive equation so that the architecture would be able to find out the constitutive model and its parameters, and provide the complete rheological behaviour of the fluid. In conclusion, we believe that viscoelastic ordering has yet to attract significant interest because of the inherent challenges of handling, modelling, and understanding the interplay between fluid rheology, confinement, flow conditions leading to the desired phenomenology. Once these aspects have been clarified, however, this technique is expected to be widely used in a variety of applications.

Data availability statement

No new data were created or analysed in this study.

Acknowledgments

F D G acknowledges support from BBSRC Grant reference BB/Y513337/1.

Conflict of interest

The authors do not declare any conflict of interest.

ORCID iDs

Francesco Del Giudice https://orcid.org/0000-0002-9414-6937
Gaetano D'Avino https://orcid.org/0000-0002-0333-6330

References

[1] Del Giudice F, D'Avino G and Maffettone P L 2021 *Lab Chip* **21** 2069–94
[2] Amini H, Lee W and Di Carlo D 2014 *Lab Chip* **14** 2739–61
[3] Yuan D, Zhao Q, Yan S, Tang S Y, Alici G, Zhang J and Li W 2018 *Lab Chip* **18** 551–67
[4] Manshadi M K D, Mohammadi M, Monfared L K and Sanati-Nezhad A 2019 *Biotechnol. Bioeng.* **117** 580–92
[5] Zhou J and Papautsky I 2020 *Microsyst. Nanoeng.* **6** 1–24
[6] Battat S, Weitz D A and Whitesides G M 2022 *Chem. Rev.* **122** 6921–37
[7] Di Carlo D, Irimia D, Tompkins R G and Toner M 2007 *Proc. Natl Acad. Sci* **104** 18892–7
[8] Kahkeshani S, Haddadi H and Di Carlo D 2016 *J. Fluid Mech.* **786** R3
[9] Kemna E W, Schoeman R M, Wolbers F, Vermes I, Weitz D A and Van Den Berg A 2012 *Lab Chip* **12** 2881–7
[10] Edd J F, Di Carlo D, Humphry K J, Köster S, Irimia D, Weitz D A and Toner M 2008 *Lab Chip* **8** 1262–4
[11] Lagus T P and Edd J F 2013 *RSC Adv.* **3** 20512–22
[12] Del Giudice F, D'Avino G, Greco F, Maffettone P L and Shen A Q 2018 *Phys. Rev. Appl.* **10** 064058
[13] D'Avino G and Maffettone P L 2019 *Microfluid. Nanofluid.* **23** 82
[14] Jeyasountharan A, Shahrivar K, D'Avino G and Del Giudice F 2021 *Anal. Chem.* **93** 5503–12
[15] Liu L, Xu H, Xiu H, Xiang N and Ni Z 2020 *Analyst* **145** 5128–33
[16] Jeyasountharan A, D'Avino G and Del Giudice F 2022 *Phys. Fluids* **34** 042015
[17] Shahrivar K and Del Giudice F 2021 *Soft Matter* **17** 8068–77
[18] Recktenwald S M, Rashidi Y, Graham I, Arratia P E, Del Giudice F and Wagner C 2024 *Soft Matter* **20** 4950–63
[19] Shahrivar K and Del Giudice F 2022 *Soft Matter* **18** 5928–33
[20] Colby R H 2010 *Rheol. Acta* **49** 425–42
[21] Del Giudice F, Calcagno V, Esposito Taliento V, Greco F, Netti P A and Maffettone P L 2017 *J. Rheol.* **61** 13–21
[22] Maisto A, McDowall D, Adams D J and Del Giudice F 2022 *ACS Appl. Eng. Mater.* **1** 258–67
[23] D'Avino G, Hulsen M A and Maffettone P L 2013 *Comput. Fluids* **86** 45–55
[24] D'Avino G and Maffettone P L 2020 *Meccanica* **55** 317–30
[25] Hu X, Chen W, Lin J, Xia Y and Yu Z 2022 *Phys. Fluids* **34** 113101
[26] Jeyasountharan A and Giudice F D 2023 *Micromachines* **14** 563
[27] Hu X, Lin P, Lin J, Zhu Z and Yu Z 2022 *J. Fluid Mech.* **936** A5
[28] D'Avino G and Maffettone P L 2022 *Electrophoresis* **43** 2206–16
[29] Esposito G, D'Avino G and Villone M M 2024 *Phys. Fluids* **36** 013106
[30] Lu X and Xuan X 2015 *Anal. Chem.* **87** 11523–30
[31] Kim J, Kim J Y, Kim Y, Lee S J and Kim J M 2017 *Anal. Chem.* **89** 8662–6
[32] Tai C W and Narsimhan V 2022 *Soft Matter* **18** 4613–24
[33] Langella A, Franzino G, Maffettone P, Larobina D and D'Avino G 2023 *Soft Matter* **19** 9541–9
[34] Nunes J, Tsai S, Wan J and Stone H A 2013 *J. Phys. D: Appl. Phys.* **46** 114002

[35] Yamada M, Sugaya S, Naganuma Y and Seki M 2012 *Soft Matter* **8** 3122–30
[36] Cheng Y, Yu Y, Fu F, Wang J, Shang L, Gu Z and Zhao Y 2016 *ACS Appl. Mater. Interfaces* **8** 1080–6
[37] Macosko E Z *et al* 2015 *Cell* **161** 1202–14
[38] De Micco M, D'Avino G, Trofa M, Villone M and Maffettone P L 2024 *J. Rheol.* **68** 801–813 under review
[39] Bonn D and Denn M M 2009 *Science* **324** 1401–2
[40] Coussot P 2014 *J. Non-Newtonian Fluid Mech.* **211** 31–49
[41] Chaparian E, Ardekani M N, Brandt L and Tammisola O 2020 *J. Non-Newtonian Fluid Mech.* **284** 104376
[42] Kordalis A, Pema D, Androulakis S, Dimakopoulos Y and Tsamopoulos J 2023 *Phys. Rev. Fluids* **8** 083301
[43] Firouznia M, Metzger B, Ovarlez G and Hormozi S 2018 *J. Non-Newtonian Fluid Mech.* **255** 19–38
[44] Lee W, Amini H, Stone H A and Di Carlo D 2010 *Proc. Natl Acad. Sci.* **107** 22413–8
[45] Hur S C, Tse H T K and Carlo D D 2010 *Lab Chip* **10** 274–80
[46] Schaaf C and Stark H 2020 *Eur. Phys. J.* E **43** 50
[47] Gupta A, Magaud P, Lafforgue C and Abbas M 2018 *Phys. Rev. Fluids* **3** 114302
[48] Hu X, Lin J and Ku X 2019 *Phys. Fluids* **31** 073306
[49] Yang S, Kim J Y, Lee S J, Lee S S and Kim J M 2011 *Lab Chip* **11** 266–73
[50] Lim E J, Ober T J, Edd J F, Desai S P, Neal D, Bong K W, Doyle P S, McKinley G H and Toner M 2014 *Nat. Commun.* **5** 4120
[51] Nam J, Lim H, Kim D, Jung H and Shin S 2012 *Lab Chip* **12** 1347
[52] Lu X, Zhu L, Hua R and Xuan X 2015 *Appl. Phys. Lett.* **197** 264102
[53] D'Avino G, Hulsen M A, Greco F and Maffettone P L 2019 *J. Non-Newtonian Fluid Mech.* **263** 33–41
[54] Tai C W, Wang S and Narsimhan V 2020 *J. Fluid Mech.* **895** A6
[55] Tai C, Wang S and Narsimhan V 2020 *AIChE J.* **66** 1–14
[56] Del Giudice F, Greco F, Netti P A and Maffettone P L 2016 *Biomicrofluidics* **10** 043501
[57] Del Giudice F, Sathish S, D'Avino G and Shen A Q 2017 *Anal. Chem.* **89** 13146–59
[58] Hu H H, Patankar N A and Zhu M Y 2001 *J. Comput. Phys.* **169** 427–62
[59] Li Z and Song P 2012 *Commun. Comput. Phys.* **12** 515–27
[60] Liu Z, Tian F B and Feng X 2022 *Comput. Methods Appl. Mech. Engrg.* **392** 114662
[61] Brooks A N and Hughes T J R 1982 *Comput. Meth. Appl. Mech. Eng.* **32** 199–259
[62] Fattal R and Kupferman R 2004 *J. Non-Newtonian Fluid Mech.* **123** 281–5
[63] Hulsen M A, Fattal R and Kupferman R 2005 *J. Non-Newtonian Fluid Mech.* **127** 27–39
[64] De Micco M, D'Avino G, Trofa M, Villone M M and Maffettone P L 2024 *J. Rheol.* **68** 801–13